SI Appendix

mRNA Binding-Protein Tristetraprolin is Essential for Cardiac Response to Iron Deficiency By Regulating Mitochondrial Function

Running title: Tristetraprolin and Mitochondrial Function

Tatsuya Sato[a,1], Hsiang-Chun Chang[a,1], Marina Bayeva[a], Jason S. Shapiro[a], Lucia Ramos-Alonso[b], Hidemichi Kouzu[a], Xinghang Jiang[a], Ting Liu[a], Sumeyye Yar[a], Konrad T. Sawicki[a], Chunlei Chen[a], María Teresa Martínez-Pastor[c], Deborah J. Stumpo[d], Paul T. Schumacker[e], Perry J. Blackshear[d], Issam Ben-Sahra[f], Sergi Puig[b], Hossein Ardehali[a,2]

[a]Feinberg Cardiovascular Research Institute, [e]Department of Pediatrics, and [f]Department of Biochemistry and Molecular Genetics, Feinberg School of Medicine, Northwestern University, Chicago, IL 60611, USA

[b]Departamento de Biotecnología, Instituto de Agroquímica y Tecnología de Alimentos, Consejo Superior de Investigaciones Científicas, 46980 Paterna, Valencia, Spain

[c]Departamento de Bioquímica y Biología Molecular, Universitat de València, 46100 Burjassot, Valencia, Spain

[d]Signal Transduction Laboratory, National Institute of Environmental Health Sciences, Research Triangle Park, NC 27709, USA

[1]These authors contributed equally to the work.

[2]To whom correspondence should be addressed:

Hossein Ardehali, MD, PhD

Tarry 14-733, 303 E Chicago Ave, Chicago, IL 60611

Phone: 312-503-2342

Fax: 312-503-0137

E-mail: h-ardehali@northwestern.edu

www.pnas.org/cgi/doi/10.1073/pnas.21804701115

SI Appendix Index:

SI Methods

Cell culture, gene downregulation, overexpression and iron chelator treatment. MEFs and H9c2 cells were grown in Dulbecco's Modified Eagle's Medium (Corning) supplemented with 10% FBS (Atlanta Biologicals), and were treated with 50 μM and 80 μM of BPD, respectively, when indicated. *Ttp* KO MEFs were generated as previously described (1). *Arnt* KO MEFs and *Irp2* KO MEFs were a generous gift from Dr. Celeste Simon (University of Pennsylvania) and Dr. Tracey A. Rouault (National Institutes of Health), respectively. siRNA against mouse *Irp1* (QIAGEN), rat *Ttp* (QIAGEN), and rat *Uqcrfs1* (Dharmacon) were used and transfected by using Dharmafect I Transfection Reagent (Dharmacon) according to the manufacturer's protocols. The siRNA concentration of 25 nM was used for single gene knockdown, while 22 nM *Ttp* siRNA and 3 nM *Uqcrfs1* siRNA were used for double-knockdown experiment. Transfection was performed 24 h before adding iron chelator when indicated. Wildtype or zinc finger dead TTP mutant plasmid were transfected into H9c2 cells using Lipofectamine 2000 (Life Technologies) according to manufacturer's instructions.

Mouse strain and iron deficiency diet. *Ttp*$^{f/f}$, *Tnfr1/2*$^{-/-}$ and *Tnfr1/2*$^{-/-}$/*Ttp*$^{-/-}$ mice were obtained from Dr. Perry Blackshear. Mice were housed in the barrier facility at Northwestern University with 12 h light and 12 h dark cycle, and received either normal chow or iron deficient diet containing 2-6 ppm of iron (TD 80394, Harlan-Teklad), which was started on the day of weaning and continued for 6 weeks. All animal studies were approved by the Institutional Animal Care and Use Committee at Northwestern University and were performed in accordance with guidelines from the National Institutes of Health.

***In silico* analysis of AU-rich elements.** AREs were identified by either of the following two criteria: 1) curated ARE entry in the ARESite Database (2), or 2) presence of AUUUA sequence in 3'UTR region of reference mRNA sequences by manual search.

RNA isolation, reverse transcription and quantitative RT PCR. RNA was isolated from cells or tissues using RNA-STAT60 (Teltest). Reverse transcription was carried out using qScript Reverse Transcription Kit (Quanta). The resulting cDNA was amplified quantitatively using PerfeCTa SYBR Green Mix (Quanta) on a 7500 Fast Real-time PCR System (Applied Biosystems). The relative gene expression was determined using differences in Ct values between gene of interest and house-keeping control genes, which are *Actb*, *Hprt1*, and/or *18S*, depending on the experiment.

mRNA stability assay and RNA co-IP. Cells were treated with 7.5 μM actinomycin D (Sigma) for indicated times and RNA was harvested and processed as described above. RNA Co-IP experiments were conducted as described previously (1).

Mitochondria isolation. Mitochondria from tissue and cells were isolated using Mitochondria Isolation Kit for Tissues and Mitochondria Isolation Kit for Cultured Cells (Pierce), respectively. For respiration assay, mitochondria from the heart were isolated as described previously (3).

Western blots and blue native gel electrophoresis. Cells and tissue were lysed in radioimmunoprecipitation assay (RIPA) buffer supplemented with protease inhibitor. Protein concentration in samples was determined using BCA Protein Quantification Kit (Pierce). Equal

amounts of protein were loaded on a tris-glycine polyacrylamide gel (Life Technologies) and transferred to nitrocellulose membrane. After blocking with TBS containing 0.005% Tween 20 and 5% milk, the membrane was incubated with primary antibody against TTP (purchased from Dr. William Rigby, Dartmouth University), NDUFS1, UQCRFS1 (Abcam), VDAC (Santa Cruz), and tubulin (Abcam) overnight. Samples for blue native gel electrophoresis were extracted with 1% n-dodecyl-β-d-maltoside (DDM) or 1.5% digitonin. The protein concentrations were determined using BCA Protein Quantification Kit (Pierce). Equal amount of proteins were loaded onto a Native PAGE Bis-Tris Protein Gel (Life Technologies) according to manufacturer's instructions. For western blotting of blue native gels, proteins were transferred onto a PVDF membrane.

Mitochondrial Aconitase activity measurements. Aconitase activity of mitochondria isolated from cells and tissues was measured using Aconitase Enzyme Activity Microplate Assay Kit (Abcam) according to manufacturer's instructions. The activities were normalized to citrate synthase activity of the same sample.

Complex III and citrate synthase activity measurements. Complex III and citrate synthase activity were measured according to previously published protocols (4).

Mitochondrial DNA content determination. Total cellular DNA from cells and tissue were isolated using Genejet Genomic DNA Purification Kit (Thermo Fisher) according to manufacturer's instructions. Following isolation, nuclear and mitochondrial DNA were quantified using quantitative realtime PCR with primers specific for 18s genomic DNA or MT-CO1 locus on mitochondrial chromosome, as described above.

Staining for mitochondrial morphology and membrane potential. Cells were stained with 250 nM of Mitotracker Green (Life Technology), 10 nM of TMRE (Life Technology), and Hoechst 33342 (Life Technology), and imaged on a Zeiss AxioObserver.Z1 microscope. The images were quantified using ImageJ.

Cell Death Analysis. Cells were stained with 5 μg/ml PI and in HBSS (Life Technologies) and Hoechst 33342 for nuclei counter stain. Images were acquired on a Zeiss AxioObserver.Z1 microscope, and cell death is defined as the number of PI-positive nuclei over total number of nuclei.

ATP content analysis. Snap-frozen heart tissue was homogenized in RIPA buffer. Cultured cells were lysed in RIPA buffer. ATP levels in the lysates were measured using ATP Bioluminescence Assay Kit CLS II (Roche), and the measured values were normalized to protein content of the same sample.

Metabolomics analysis. Snap-frozen heart tissue was homogenized in 1.5ml 80% HPLC-grade methanol (Fisher Scientific). Protein fraction were separated via centrifugation and reextrracted twice with 750μl of 80% HPLC-grade methanol. Samples were then dried under nitrogen gas using an NEVAP (Organomation Associates, Inc). Insoluble protein fraction was solubilized in 10M Urea in 10mM Tris-HCl pH 8.0, and protein concentration were determined using BCA Protein Assay Kit (Pierce). Samples were analyzed by High-Performance Liquid Chromatography and High-Resolution Mass Spectrometry and Tandem Mass Spectrometry

(HPLC-MS/MS). The sample reconstitution volumes were adjusted based on the protein concentration in the same sample, and 10 µl of the reconstituted sample were injected. Specifically, system consisted of a Thermo Q-Exactive in line with an electrospray source and an Ultimate3000 (Thermo) series HPLC consisting of a binary pump, degasser, and auto-sampler outfitted with a Xbridge Amide column (Waters; dimensions of 4.6 mm × 100 mm and a 3.5 µm particle size). The mobile phase A contained 95% (vol/vol) water, 5% (vol/vol) acetonitrile, 20 mM ammonium hydroxide, 20 mM ammonium acetate, pH = 9.0; B was 100% Acetonitrile. The gradient was as following: 0 min, 15% A; 2.5 min, 30% A; 7 min, 43% A; 16 min, 62% A; 16.1-18 min, 75% A; 18-25 min, 15% A with a flow rate of 400 µL/min. The capillary of the ESI source was set to 275 °C, with sheath gas at 45 arbitrary units, auxiliary gas at 5 arbitrary units and the spray voltage at 4.0 kV. In positive/negative polarity switching mode, an m/z scan range from 70 to 850 was chosen and MS1 data was collected at a resolution of 70,000. The automatic gain control (AGC) target was set at 1 × 106 and the maximum injection time was 200 ms. The top 5 precursor ions were subsequently fragmented, in a data-dependent manner, using the higher energy collisional dissociation (HCD) cell set to 30% normalized collision energy in MS2 at a resolution power of 17,500. Data acquisition and analysis were carried out by Xcalibur 4.0 software and Tracefinder 2.1 software, respectively (both from Thermo Fisher Scientific).

Oxygen consumption. Oxygen consumption rate of intact cells was measured using Seahorse XF24 Bioanalyzer according to the manufacturer's instructions. The number of $15x10^3$ cells were placed in each well. Oxygen consumption of isolated mitochondria was measured using Seahorse XFe96 Bioanalyzer. 1µg and 0.25µg of mitochondria in 20µl of MAS buffer (70 mM sucrose, 220 mM mannitol, 5 mM KH_2PO_4, 5 mM $MgCl_2$, 5 mM, 2 mM HEPES, 1 mM EGTA, 0.2% fatty acid-free BSA, pH 7.4) were loaded in each well for pyruvate/malate-driven

respiration and succinate-driven respiration, respectively. The plates were centrifuged at 2000g for 20 minutes. Following centrifugation, MAS buffer containing 5 mM pyruvate and malate or 5mM sodium succinate and 2μM rotenone were added to a final volume of 180μl and incubated for 8 min at 37 °C without CO_2. Oxygen tension was measured in the Seahorse XFe96 Bioanalyzer at baseline and following injections of 50 mM ADP, 33 μM oligomycin, 80 μM carbonyl cyanide 3-chlorophenylhydrazone (CCCP), and 45.6 μM antimycin.

^{55}Fe incorporation into UQCRFS1. ^{55}Fe-NTA was prepared as described previously (1). Cells were preincubated with 280 nM of ^{55}Fe-NTA in complete media for 36 h. siRNA transfection, iron chelation, and mitochondria isolation were performed as described above. Mitochondria were lysed in lysis buffer (25 mM Tris-HCl pH 7.4, 150 mM NaCl, 1 mM EDTA, 1% NP-40, 5% glycerol) supplemented with protease inhibitors, and protein content was quantified using BCA protein assay kit (Pierce). Equal amount of protein from each sample were incubated with monoclonal antibody against UQCRFS1 (Abcam) or control IgG (Sigma). The antibody bound proteins were purified using protein G agarose beads (Roche). The beads were washed with washing buffer (25 mM Tris-HCl pH 7.4, 150 mM NaCl, 1 mM EDTA, 0.1% NP-40, 5% glycerol), and the radioactivity bound to the beads was counted using liquid scintillation counting. Total UQCRFS1 content in the mitochondrial lysate was determined using western blotting as described above and served as normalization for bead-bound radioactivity.

ROS measurements. Isolated mitochondria were resuspended in buffer containing 220mM mannitol, 75 mM sucrose, 20 mM HEPES (pH 7.4), 0.5 mM EDTA, 0.1 mM ATP, 0.5 mM magnesium acetate. Mitochondria were fueled with 10 mM succinate or 3 mM L-glutamic acid and 3mM sodium malate. ROS production was measured as described previously (5). When

indicated, rotenone, antimycin A, myxothiazol (Sigma) were used at 20 μM, 20 μM, and 20 μM, respectively. Tissue ROS level was determined using the LPO microplate-based assay kit (Oxford Biochemical Research) according to the manufacturer's instructions. Mitochondrial ROS in intact cells was measured using MitoSOX dye (Life Technology) as described previously (6).

Cellular iron quantification. Total, cytosolic, and mitochondrial iron were quantified as previously described (7).

Echocardiography, organ harvest, and histological analysis. Parasternal short- and long-axis views of the heart were obtained using a Vevo 770 high-resolution imaging system with a 30 MHz scan head. 2D and M-mode images were obtained and analyzed. Cardiac function was calculated as previously described (8). At the time of tissue harvest, mice were anesthetized with 250 mg/kg dose of freshly prepared Tribromoethanol (Avertin) and tissue was excised and rinsed in phosphate buffered saline to remove excess blood. The heart tissue for biochemical assays was then freshly frozen in liquid nitrogen and stored at -80 °C until the assay. For histological analysis, the heart tissue after rinse was fixed overnight in 4% paraformaldehyde before graded dehydration in 70%, 80%, 90% and 100% ethanol. The tissue sample was further dehydrated with xylene and embedded into paraffin. Sections were stained with hematoxylin and eosin for evaluation of general cardiac morphology and tissue organization. Masson's Trichrome staining was used to visualize cardiac fibrosis.

Yeast Experiments. To measure oxygen consumption rates, yeast *cth1*Δ*cth2*Δ mutant strain was transformed with pRS416 (Vector), pSP410 (pRS416-*CTH2*), pSP449 (p416TEF-*Flag2-CTH2*), or pSP450 (p416TEF-*Flag2-CTH2-C190R*) plasmids (1, 9). Yeast transformants were

grown for 6 hours in synthetic medium lacking uracil (SC-ura) to maintain the plasmids and supplemented with 10 μM $Fe(NH_4)_2(SO_4)_2$ (ferrous ammonium sulfate, FAS) or 100 μM bathophenanthroline disulfonic acid disodium (BPS, a specific Fe^{2+}-chelator) to obtain iron-sufficient and iron-deficient conditions, respectively. The cells contained in a volume of culture corresponding to 1.5 OD_{600} units were washed with sterile distilled H_2O, resuspended in respiratory YPEG medium (1% yeast extract, 2% peptone, 2% ethanol, 3% glycerol), and transferred to an air-tight chamber. Oxygen content was monitored for at least 10 min using a Clark-type O_2 electrode from Hansatech (Oxyview system). The rate of decrease in oxygen content, related to the amount of cells (nmol O_2/OD_{600}/min), was taken as index of the respiratory ability. To determine *S. cerevisiae* mRNA levels, yeast *cth1Δcth2Δ* mutant strain was transformed with pRS416 (Vector), pSP410 (pRS416-*CTH2*), pSP474 (pRS416-*CTH2p-hTTP-CYC1t*), or pSP475 (pRS416-*CTH2p-hTTP-C124R-CYC1t*) plasmids (1). Yeast transformants were grown for 6 hours in synthetic medium lacking uracil (SC-ura) to maintain the plasmids and supplemented with 10 μM $Fe(NH_4)_2(SO_4)_2$ (ferrous ammonium sulfate, FAS) or 100 μM bathophenanthroline disulfonic acid disodium (BPS, a specific Fe^{2+}-chelator) to obtain iron-sufficient and iron-deficient conditions, respectively. Total mRNA was extracted and analyzed by quantitative reverse transcription PCR (qPCR) as previously described (10).

Statistical analysis. Experiments in immortalized cell lines (MEFs and H9c2s) were performed in triplicate for each condition, and each experiment was replicated at least once. Experiments using rat neonatal cardiomyocytes (NRCMs) were performed in triplicate for each heart. For *in vivo* experiments, animals were assigned to experimental groups using simple randomization, without investigator blinding. No statistical methods were used to predetermine sample size. Unpaired two-tailed Student's t-tests or one-way ANOVA were used to determine statistical

significance. $P < 0.05$ was considered to be statistically significant, as indicated by an asterisk. Significant one-way ANOVA is followed by Tukey post hoc analysis.

References

1. Bayeva M*, et al.* (2012) mTOR regulates cellular iron homeostasis through tristetraprolin. *Cell Metab* 16(5):645-657.
2. Gruber AR, Fallmann J, Kratochvill F, Kovarik P, & Hofacker IL (2011) AREsite: a database for the comprehensive investigation of AU-rich elements. *Nucleic acids research* 39(Database issue):D66-69.
3. Rines AK*, et al.* (2017) Snf1-related kinase improves cardiac mitochondrial efficiency and decreases mitochondrial uncoupling. *Nature communications* 8:14095.
4. Spinazzi M, Casarin A, Pertegato V, Salviati L, & Angelini C (2012) Assessment of mitochondrial respiratory chain enzymatic activities on tissues and cultured cells. *Nature protocols* 7(6):1235-1246.
5. Chang HC*, et al.* (2016) Reduction in mitochondrial iron alleviates cardiac damage during injury. *EMBO molecular medicine* 8(3):247-267.
6. Khechaduri A, Bayeva M, Chang HC, & Ardehali H (2013) Heme levels are increased in human failing hearts. *Journal of the American College of Cardiology* 61(18):1884-1893.
7. Ichikawa Y*, et al.* (2012) Disruption of ATP-binding cassette B8 in mice leads to cardiomyopathy through a decrease in mitochondrial iron export. *Proceedings of the National Academy of Sciences of the United States of America* 109(11):4152-4157.
8. Ichikawa Y*, et al.* (2014) Cardiotoxicity of doxorubicin is mediated through mitochondrial iron accumulation. *The Journal of clinical investigation* 124(2):617-630.
9. Puig S, Vergara SV, & Thiele DJ (2008) Cooperation of two mRNA-binding proteins drives metabolic adaptation to iron deficiency. *Cell metabolism* 7(6):555-564.
10. Sanvisens N*, et al.* (2014) Yeast Dun1 kinase regulates ribonucleotide reductase inhibitor Sml1 in response to iron deficiency. *Molecular and cellular biology* 34(17):3259-3271.

Fig. S1

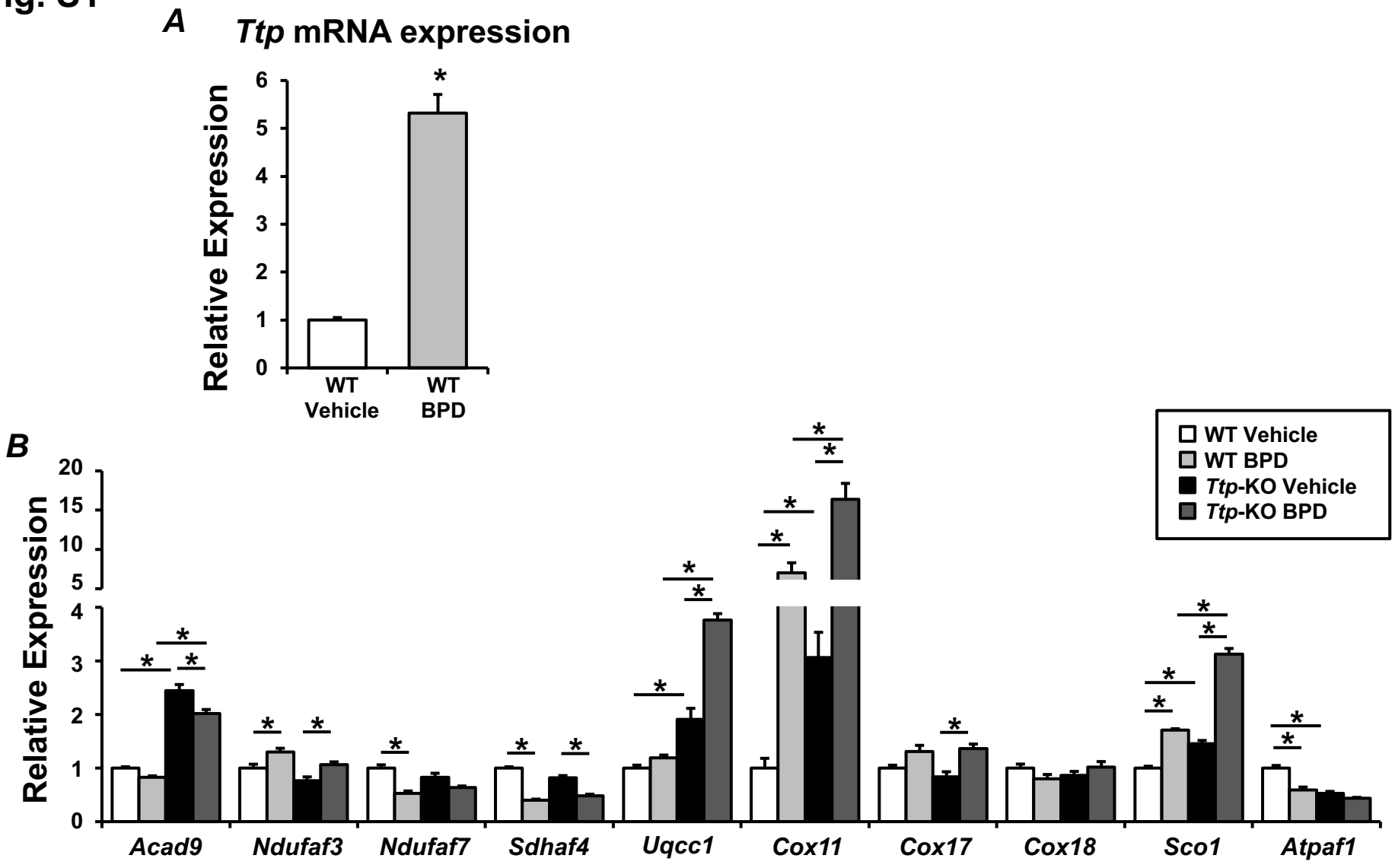

Fig. S1. mRNA levels of *Ttp* and mitochondrial ETC proteins in response to iron chelation. (*A*) *Ttp* mRNA in response to BPD. (*B*) mRNA levels of assembly factors in mitochondrial ETC in WT and *Ttp* KO MEFs in the presence and absence of BPD. $n = 6$. All graphs show mean ± s.e.m. *$P < 0.05$ by ANOVA with Tukey post hoc analysis for each gene.

Fig. S2

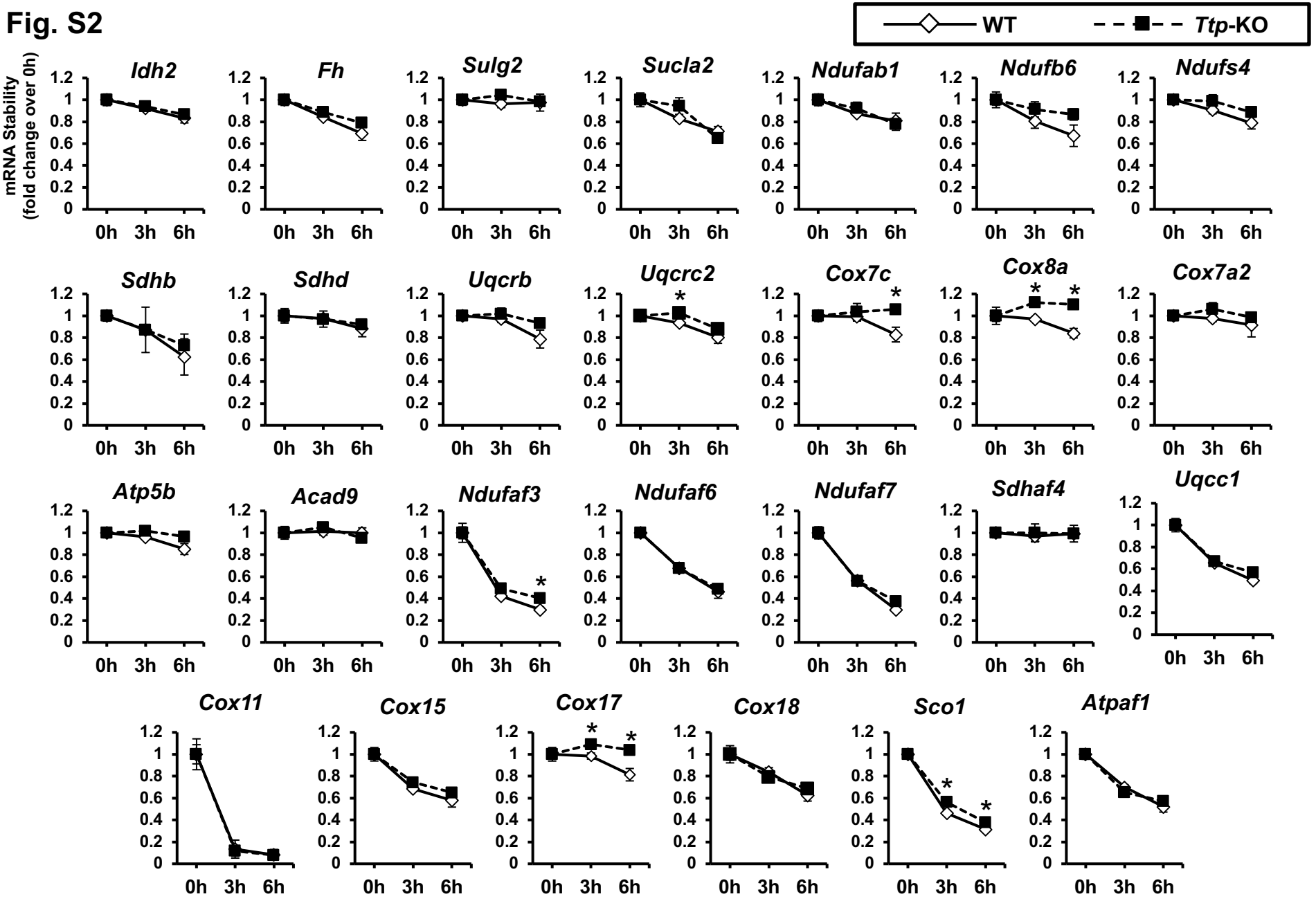

Fig. S2. mRNA decay studies of the ETC and TCA cycle genes that are potentially targeted by TTP based on the *in silico* analysis. n = 6. Data presented as mean ± s.e.m. **P* < 0.05 by unpaired Student's t test.

Fig. S3

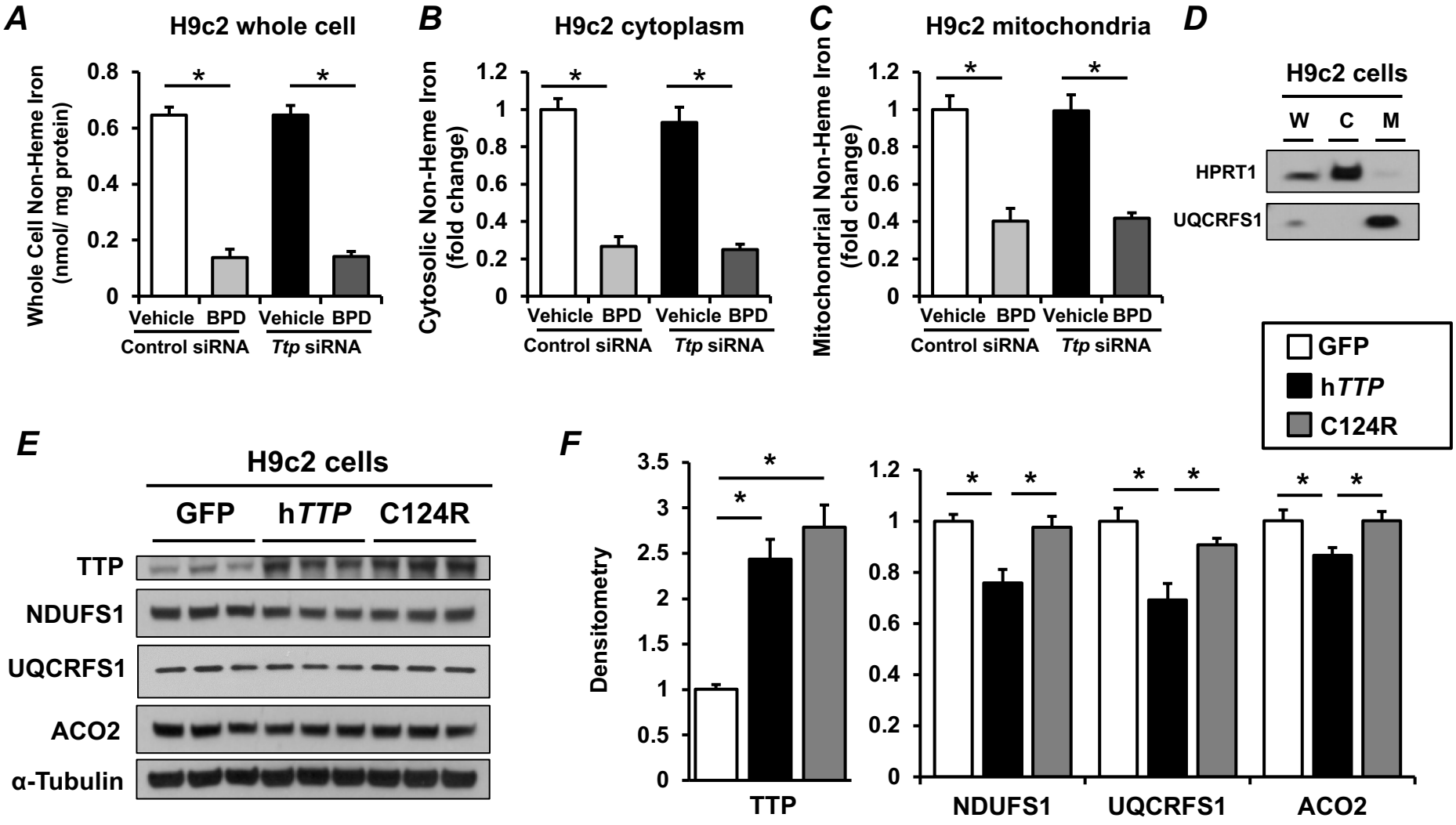

Fig. S3. TTP regulates *Ndufs1*, *Uqcrfs1*, and *Aco2* in cultured cardiomyocytes. (*A-C*) Non-heme iron in whole cell (*A*), cytoplasm (*B*), and mitochondria (*C*) of H9c2 cells in the presence and absence of iron deficiency. (*D*) Western blot confirming the purity of mitochondrial isolation. W= whole cell; C = cytoplasm; M = mitochondria. (*E*) Western blot of TTP, NDUFS1, UQCRFS1, and ACO2 in H9c2 cells with overexpression of WT human TTP (h*TTP*) or mutant form with mutation in the TZF domain (C124R). (*F*) Summary bar graph of the Western blot. *n* = 6 for panels *A-C* and n = 3 for panel *F*. All graphs show mean ± s.e.m. **P* < 0.05 by ANOVA with Tukey post hoc analysis.

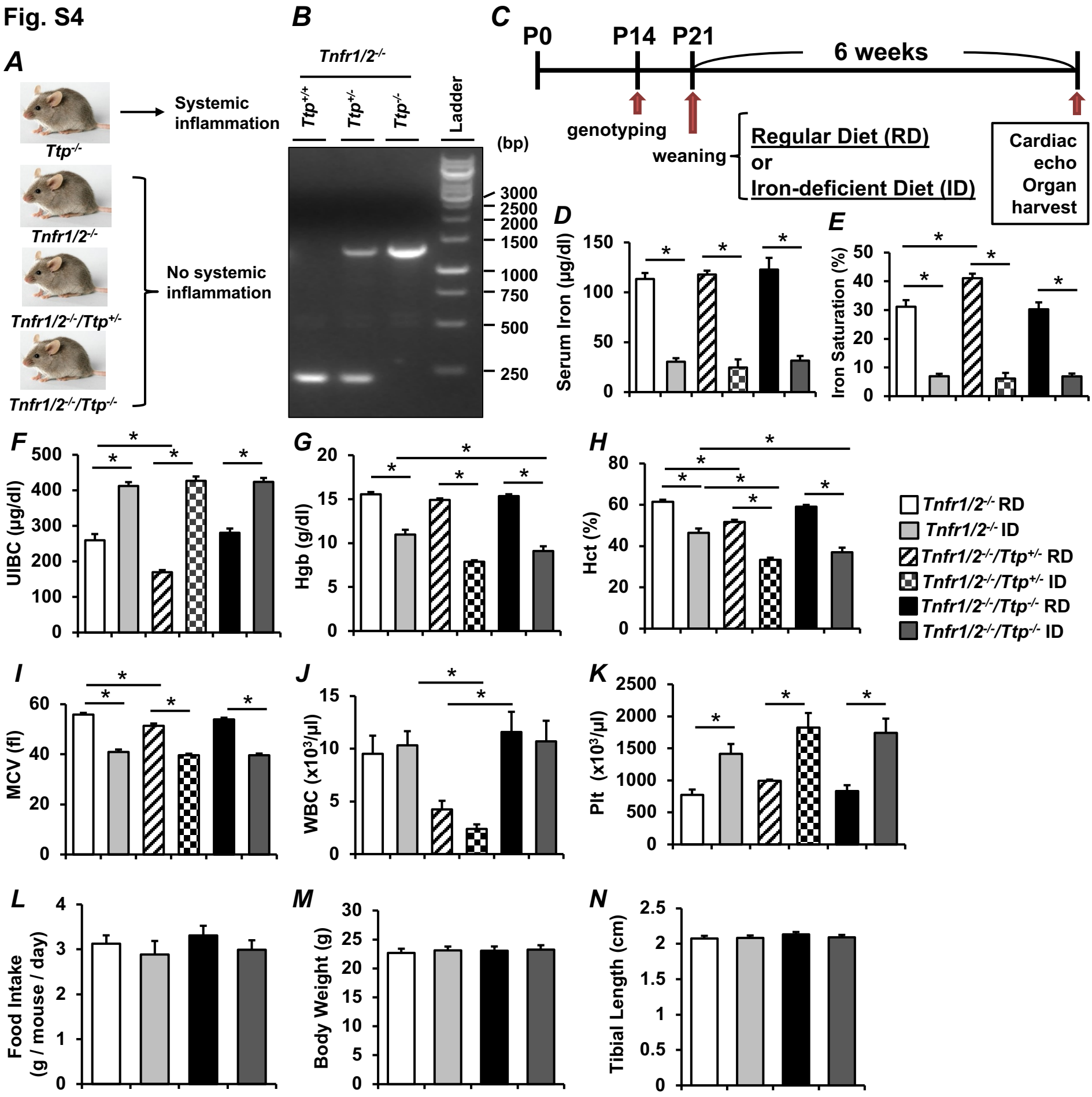
Fig. S4
A
Ttp-/-
Systemic inflammation
Tnfr1/2-/-
Tnfr1/2-/-/Ttp+/-
No systemic inflammation
Tnfr1/2-/-/Ttp-/-
B
Tnfr1/2-/-
Ttp+/+
Ttp+/-
Ttp-/-
Ladder
(bp)
3000
2500
2000
1500
1000
750
500
250
C
P0
P14
P21
6 weeks
genotyping
weaning
Regular Diet (RD)
or
Iron-deficient Diet (ID)
Cardiac echo
Organ harvest
D
Serum Iron (μg/dl)
E
Iron Saturation (%)
F
UIBC (μg/dl)
G
Hgb (g/dl)
H
Hct (%)
Tnfr1/2-/- RD
Tnfr1/2-/- ID
Tnfr1/2-/-/Ttp+/- RD
Tnfr1/2-/-/Ttp+/- ID
Tnfr1/2-/-/Ttp-/- RD
Tnfr1/2-/-/Ttp-/- ID
I
MCV (fl)
J
WBC (x10³/μl)
K
Plt (x10³/μl)
L
Food Intake (g / mouse / day)
M
Body Weight (g)
N
Tibial Length (cm)

Fig. S4. Iron deficient diet regimen induced iron deficiency in mice. (*A*) Mouse models used. The *Ttp*$^{-/-}$ mice display systemic inflammation. Thus, we used *Tnfr1/2*$^{-/-}$ (as controls), *Tnfr1/2*$^{-/-}$/*Ttp*$^{+/-}$ and *Tnfr1/2*$^{-/-}$/*Ttp*$^{-/-}$ in our studies. (*B*) PCR gel of mice confirming genotypes. This procedure was done on all mice in this study. (*C*) Protocol for inducing iron deficiency in mice. (*D*-*F*) Compared with regular diet (RD), iron deficiency (ID) diet resulted in decreased systemic iron (*D*) and iron saturation (*E*), and an increased unbound iron-binding capacity (UIBC) (*F*) to the same degree in all three genotypes. (*G*-*K*) Compared to RD, ID resulted in decreased hemoglobin (Hgb) (*G*), hematocrit (Hct) (*H*), and mean corpuscular volume (MCV) (*I*), no change in white blood cell (WBC) count (*J*), and increased platelet (Plt) count (*K*). Homozygote deletion of *Ttp* led to a greater magnitude of change in Hgb (*G*), and Hct (*H*) after ID as compared with *Ttp*-intact mice. (*L*-*N*) Food intake (*L*), body weight at the end of study (*M*), and tibial length at the time of sacrifice (*N*) of mice receiving indicated treatments. n = 6 males and 6 females. All graphs show mean ± s.e.m. *P < 0.05 by ANOVA with Tukey post hoc analysis.

Fig. S5

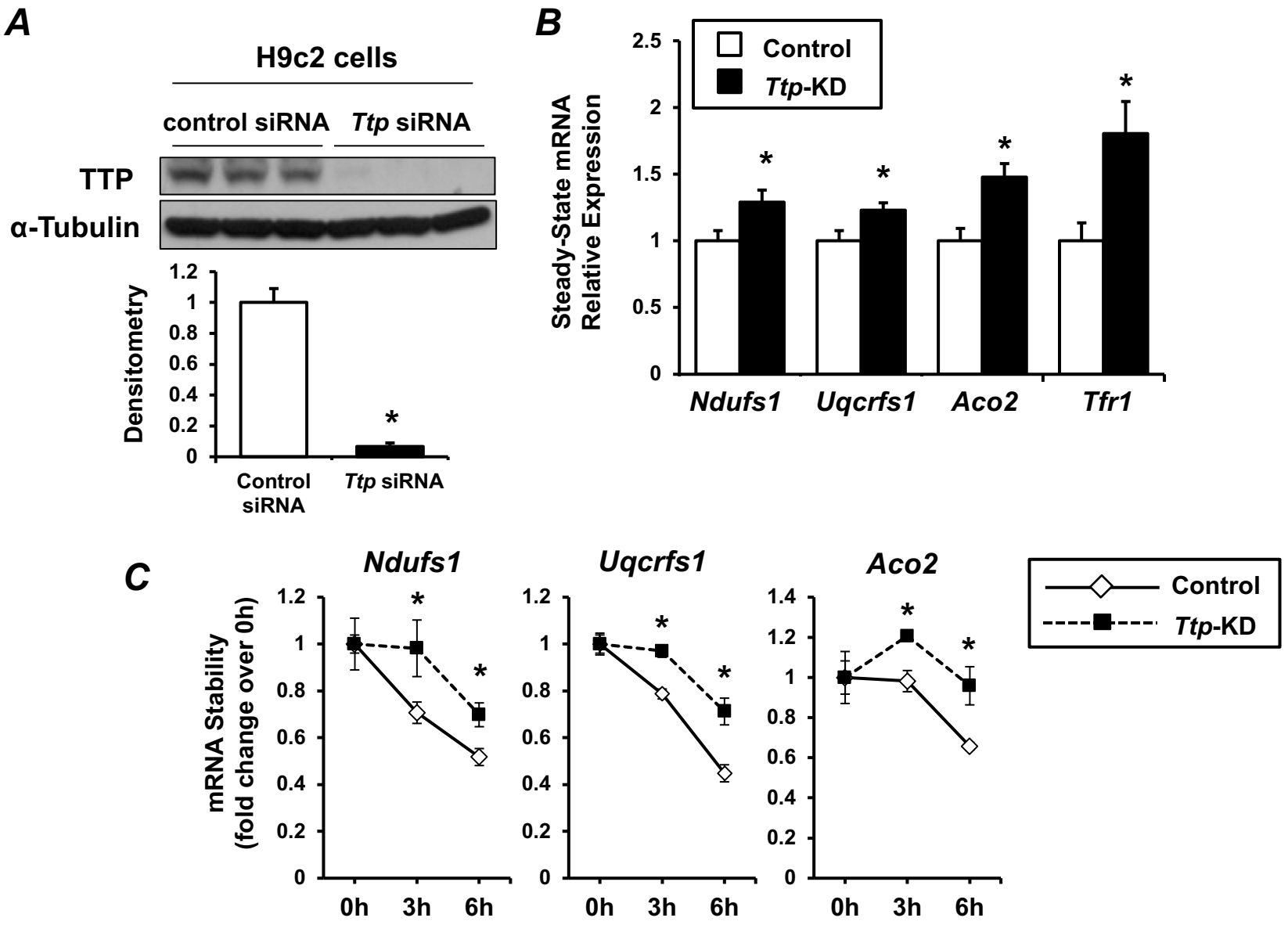

Fig. S5. Acute downregulation of *Ttp* resulted in increased mRNA levels of its targets at baseline. (*A*) Protein levels of TTP in H9c2 cells after treatment with *Ttp* siRNA. Densitometry data of TTP level is shown in the bar graph (n = 3). (*B*) Steady state mRNA levels of *Nfufs1*, *Uqcrfs1*, *Aco2*, and *Tfr1* in H9c2 cells treated with control or *Ttp* siRNA (n = 6). (*C*) mRNA decay studies of *Ndufs1*, *Uqcrfs1*, and *Aco2* in H9c2 cells treated with control or *Ttp* siRNA (n = 6). All graphs show mean ± s.e.m. *P < 0.05 by ANOVA with Tukey post hoc analysis.

Fig. S6

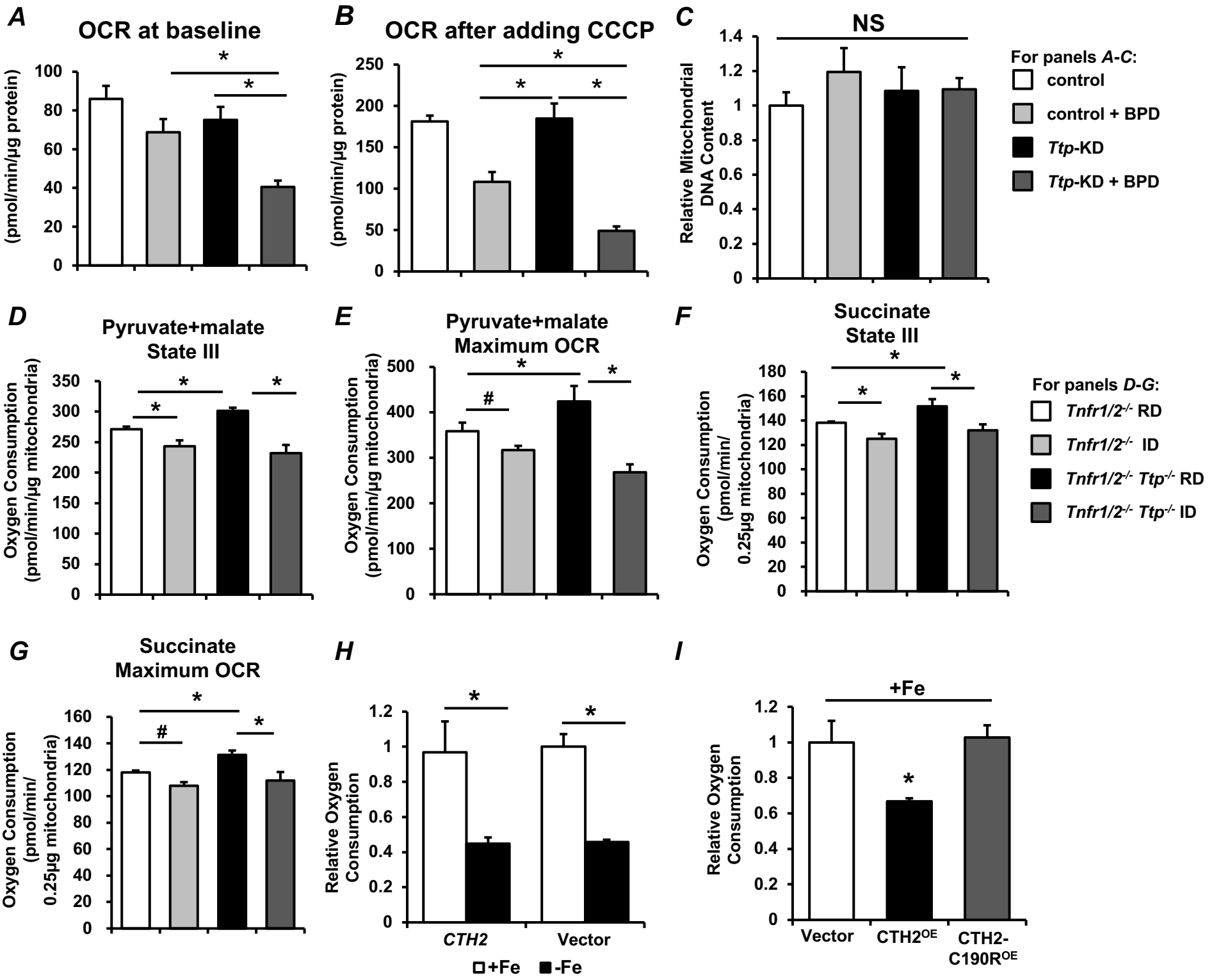
A
OCR at baseline
(pmol/min/µg protein)
B
OCR after adding CCCP
(pmol/min/µg protein)
C
NS
Relative Mitochondrial DNA Content
For panels A-C:
control
control + BPD
Ttp-KD
Ttp-KD + BPD
D
Pyruvate+malate State III
Oxygen Consumption (pmol/min/µg mitochondria)
E
Pyruvate+malate Maximum OCR
Oxygen Consumption (pmol/min/µg mitochondria)
F
Succinate State III
Oxygen Consumption (pmol/min/ 0.25µg mitochondria)
For panels D-G:
Tnfr1/2-/- RD
Tnfr1/2-/- ID
Tnfr1/2-/- Ttp-/- RD
Tnfr1/2-/- Ttp-/- ID
G
Succinate Maximum OCR
Oxygen Consumption (pmol/min/ 0.25µg mitochondria)
H
Relative Oxygen Consumption
CTH2
Vector
+Fe
-Fe
I
+Fe
Relative Oxygen Consumption
Vector
CTH2OE
CTH2-C190ROE

Fig. S6. Iron deficiency results in further reduction of mitochondrial respiration in the absence of TTP. (*A*-*B*) Oxygen consumption rate (OCR) at baseline (*A*) and after the addition of carbonyl cyanide 3-chlorophenyl hydrazine (CCCP) (*B*) as assessed by Seahorse XF24 analyzer. N=10 for panels *A* and *B*. (*C*) Mitochondrial DNA content in cells with and without *Ttp* KD in the presence and absence of iron deficiency. N=10-12 for all groups. (*D*-*E*) Pyruvate and malate driven state III respiration (*D*) and maximal respiration (*E*) in isolated mitochondria from *Tnfr1/2*$^{-/-}$ and *Tnfr1/2*$^{-/-}$*Ttp*$^{-/-}$ mice with and without iron deficiency. (*F*-*G*) Succinate driven state III respiration (*F*) and maximal respiration (*G*) in isolated mitochondria from *Tnfr1/2*$^{-/-}$ and *Tnfr1/2*$^{-/-}$*Ttp*$^{-/-}$ mice with and without iron deficiency. N=4-7 mice in each group for panels *D*-*G*. (*H*) Oxygen consumption in *cth1Δcth2Δ* yeast reconsistuted with *CTH2* or empty vector in the absence and presence of iron deficiency. (*I*) Oxygen consumption in yeast overexpressing wild type (CTH2^{OE}) or zinc-finger-dead mutant (CTH2-C190R^{OE}) driven by constitutive promoter grown under iron sufficient state. N=3 for panels *I* and *J*. All graphs show mean ± s.e.m. $^{*}P < 0.05$ and $^{\#}P < 0.1$ by ANOVA with Tukey post hoc analysis.

Fig. S7

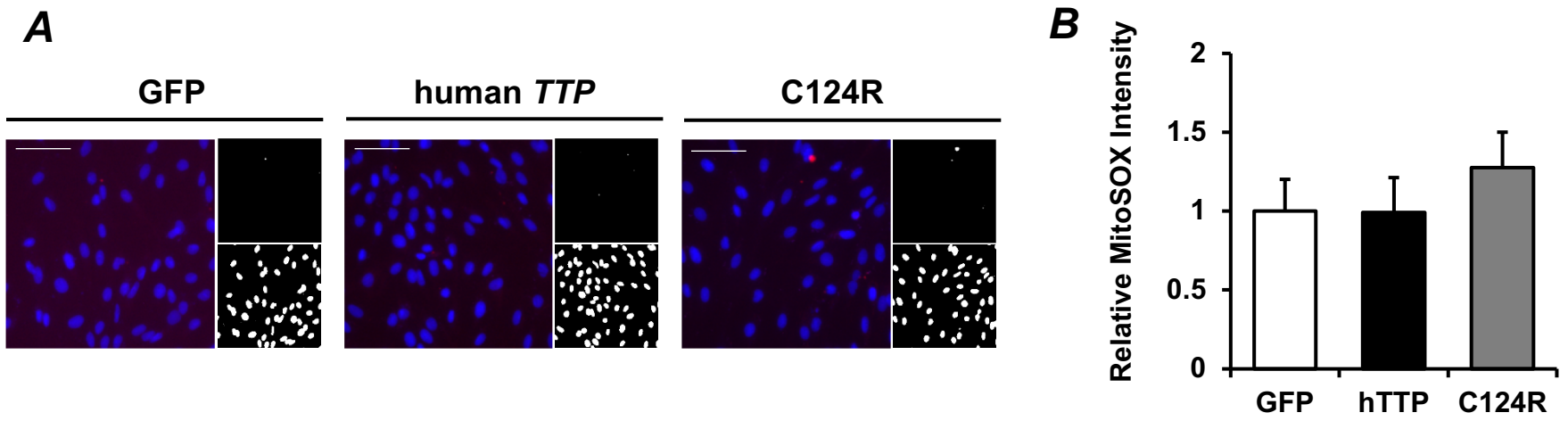

Fig. S7. The effect of TTP overexpression on mitochondrial ROS production in iron replete state. (*A*) Representative fluorescence images of MitoSOX Red staining in H9c2 cells with overexpression of vector containing GFP (as control), human *TTP*, or *TTP* C124R. White bar indicates 100 μm. Upper right panel shows positive red fluorescence signal in black and white scale and lower right shows nuclear staining by Hoechst 33342 in black and white scale. (*B*) Summary bar graph of MitoSOX intensity. $n = 4$. All graphs show mean ± s.e.m. Data analyzed with ANOVA with Tukey post hoc analysis.

Fig. S8

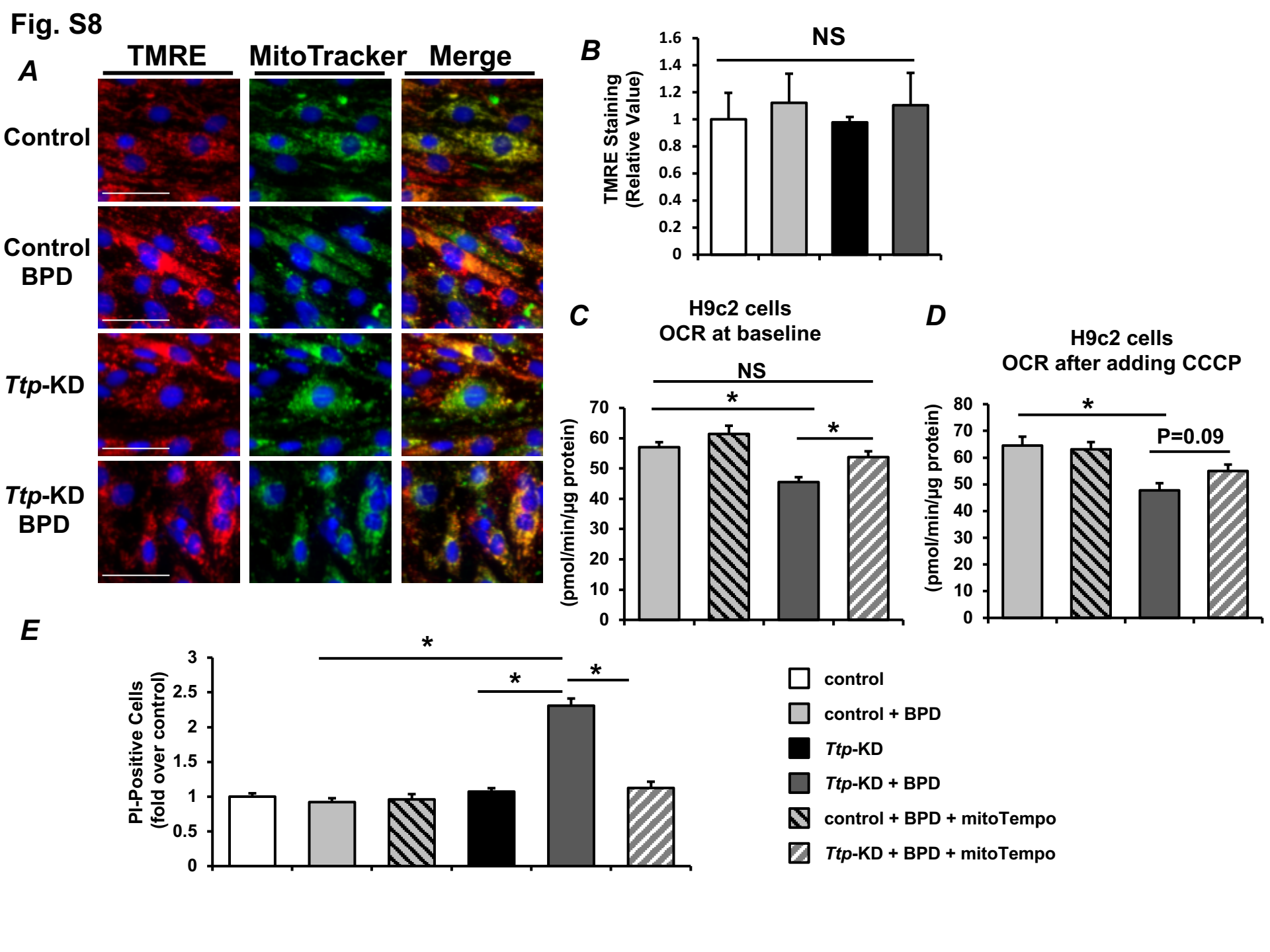
A
TMRE
MitoTracker
Merge
Control
Control BPD
Ttp-KD
Ttp-KD BPD
B
NS
TMRE Staining (Relative Value)
1.6
1.4
1.2
1
0.8
0.6
0.4
0.2
0
C
H9c2 cells
OCR at baseline
NS
*
*
(pmol/min/μg protein)
70
60
50
40
30
20
10
0
D
H9c2 cells
OCR after adding CCCP
*
P=0.09
(pmol/min/μg protein)
80
70
60
50
40
30
20
10
0
E
*
*
*
PI-Positive Cells (fold over control)
3
2.5
2
1.5
1
0.5
0
control
control + BPD
Ttp-KD
Ttp-KD + BPD
control + BPD + mitoTempo
Ttp-KD + BPD + mitoTempo

Fig. S8. ROS contributes to reduced mitochondrial oxygen consumption and increased cell death in *Ttp* KD cells under iron deficiency. (*A*) Representative images of cells receiving indicated treatment stained with 10nM TMRE and 250nM MitoTracker Green. Hoechst 33342 was used as a nuclear counterstain. (*B*) Summary of mitochondrial membrane potential as assessed by TMRE signal normalized to MitoTracker Green signal. $n = 3$ with multiple images of each sample. White bar indicates 100 μm. (*C*-*D*) OCR at baseline (*C*) and after the addition of CCCP (*D*) in iron-deficient cells with or without *Ttp* KD treated with mitochondria-targeted antioxidant. N=12 for panels *C* and *D*. (*E*) Cell death in NRCM with indicated treatment as assessed by propidium iodide (PI) staining. N=6 for panel *E*. All graphs show mean ± s.e.m. $^*P < 0.05$ by ANOVA with Tukey post hoc analysis.

Fig. S9

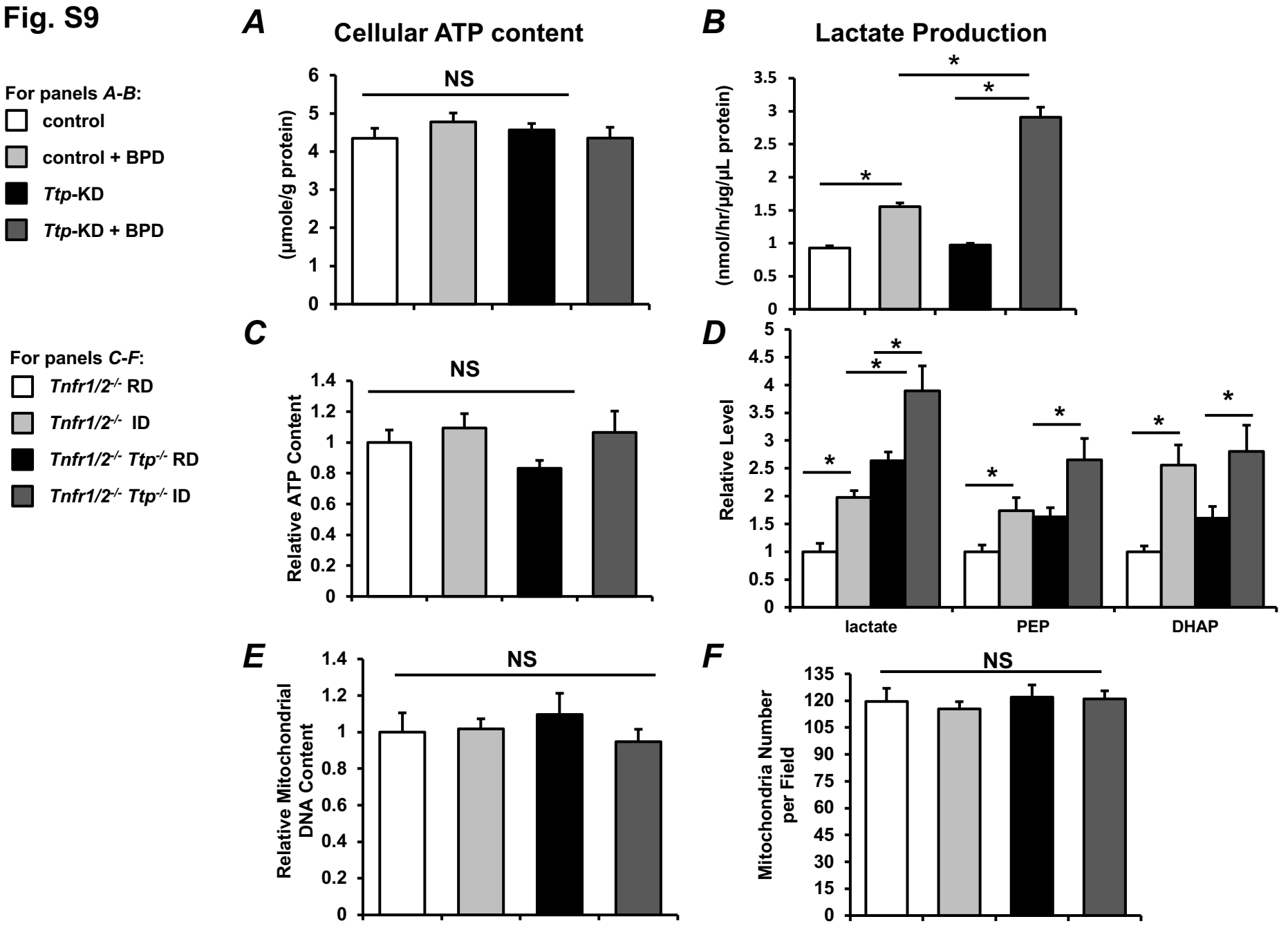
A
Cellular ATP content
NS
(µmole/g protein)
B
Lactate Production
(nmol/hr/µg/µL protein)
For panels A-B:
control
control + BPD
Ttp-KD
Ttp-KD + BPD
C
Relative ATP Content
D
Relative Level
lactate
PEP
DHAP
For panels C-F:
Tnfr1/2-/- RD
Tnfr1/2-/- ID
Tnfr1/2-/- Ttp-/- RD
Tnfr1/2-/- Ttp-/- ID
E
Relative Mitochondrial DNA Content
F
Mitochondria Number per Field

Fig. S9. Iron deficiency results in increased glycolysis in cultured cells and in mouse hearts. (*A-B*) ATP content (*A*) and lactate production (*B*) in H9c2 cells with or without *Ttp* KD and in the presence and absence of iron deficiency. n = 3 for panels *A* and *B*. (*C*) Cardiac ATP content in *Tnfr1/2*$^{-/-}$ and *Tnfr1/2*$^{-/-}$*Ttp*$^{-/-}$ mice. n=4-7 in each group. (*D*) Relative glycolytic intermediate metabolite levels in *Tnfr1/2*$^{-/-}$ and *Tnfr1/2*$^{-/-}$*Ttp*$^{-/-}$ mice with and without iron deficiency as quantified by LC/MS/MS. N=4-6 in each group. (*E-F*) Mitochondrial DNA content (*E*) and mitochondrial number (*F*) in *Tnfr1/2*$^{-/-}$ and *Tnfr1/2*$^{-/-}$*Ttp*$^{-/-}$ mice with and without iron deficiency. N=6-8 for panel *E* and 4-6 low power fields from two mice for panel *F*. All graphs show mean ± s.e.m. *$P < 0.05$ by ANOVA with Tukey post hoc analysis.

Fig. S10

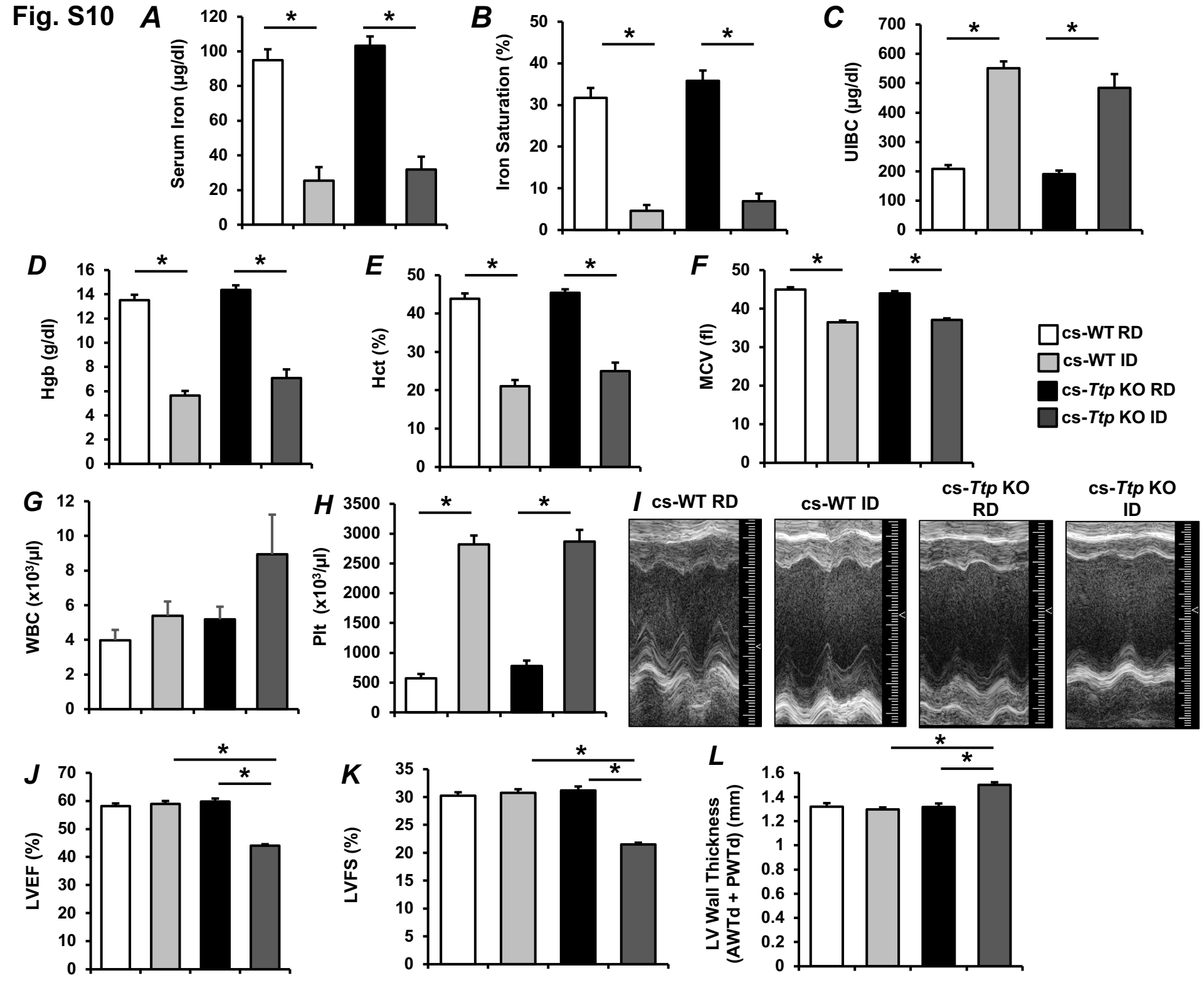
A
Serum Iron (µg/dl)
B
Iron Saturation (%)
C
UIBC (µg/dl)
D
Hgb (g/dl)
E
Hct (%)
F
MCV (fl)
cs-WT RD
cs-WT ID
cs-Ttp KO RD
cs-Ttp KO ID
G
WBC (x10³/µl)
H
Plt (x10³/µl)
I
cs-WT RD
cs-WT ID
cs-Ttp KO RD
cs-Ttp KO ID
J
LVEF (%)
K
LVFS (%)
L
LV Wall Thickness (AWTd + PWTd) (mm)

Fig. S10. Iron deficient diet regimen induced iron deficiency in cardiac-specific (cs) *Ttp* knockout mice. (*A*-*C*) Compared with regular diet (RD), iron deficiency (ID) resulted in decreased systemic iron (*A*) and iron saturation (*B*), and an increased unbound iron-binding capacity (UIBC) (*C*) to the same degree in cs-WT *and* cs-*Ttp* KO mice. (*D*-*H*) Compared to RD, ID resulted in decreased hemoglobin (Hgb) (*D*), hematocrit (Hct) (*E*), and mean corpuscular volume (MCV) (*F*), no change in white blood cell (WBC) count (*G*), and increased platelet (Plt) count (*H*). (*I*) Representative echocardiography images for cs-WT or cs-*Ttp* KO mice with indicated treatment. (*J*-*L*) Ejection fraction (EF) (*J*), fractional shortening (FS) (*K*) and left ventricular wall thickness (*L*) as measured by echocardiography cs-WT and cs-*Ttp* KO mice with and without iron deficiency. N=12-24 mice in each group. All graphs show mean ± s.e.m. $*P < 0.05$ by ANOVA with Tukey post hoc analysis.

Table S1. Mitochondrial electron transport chain and TCA cycle genes with conserved 3' UTR AUUUA motifs in mouse, rat and human genes.

Gene Symbol	Gene Name	Mouse ARE	Rat ARE	Human ARE
TCA cycle (5/9)				
Aco2	aconitase 2, mitochondrial	1	1	1
Idh2	isocitrate dehydrogenase 2 (NADP+), mitochondrial	2	2	2
Suclg2	succinate-CoA ligase, GDP-forming, beta subunit	6	4	5
Sucla2	succinate-CoA ligase, ADP-forming, beta subunit	2	2	4
Fh	fumarate hydratase	2	2	3
Complex I (4/44)				
Ndufab1	NADH dehydrogenase (ubiquinone) 1 alpha subcomplex, 13	1	3	1
Ndufb6	NADH dehydrogenase (ubiquinone) 1 beta subcomplex, 6, 17kDa	1	2	4
Ndufs1	NADH dehydrogenase (ubiquinone) Fe-S protein 1, 75kDa (NADH-coenzyme Q reductase)	1	2	8
Ndufs4	NADH dehydrogenase (ubiquinone) Fe-S protein 4, 18kDa (NADH-coenzyme Q reductase)	4	2	1
Complex II (2/4)				
Sdhb	succinate dehydrogenase complex, subunit B, iron sulfur (Ip)	1	1	2
Sdhd	succinate dehydrogenase complex, subunit D, integral membrane protein	4	2	4
Complex III (3/10)				
Uqcrb	ubiquinol-cytochrome c reductase binding protein	1	3	12
Uqcrc2	ubiquinol-cytochrome c reductase core protein II	2	1	1
Uqcrfs1	ubiquinol-cytochrome c reductase, Rieske iron-sulfur polypeptide 1	2	2	1
Complex IV (3/19)				
Cox7a2	cytochrome c oxidase subunit VIIa polypeptide 2 (liver)	2	2	1
Cox7c	cytochrome c oxidase subunit VIIc	1	2	1
Cox8a	cytochrome c oxidase subunit VIIIA (ubiquitous)	1	1	1
Complex V (1/19)				
Atp5b	ATP synthase, H+ transporting, mitochondrial F1 complex, beta polypeptide	4	1	1
Assembly Factors (13/38)				
Acad9	acyl-CoA dehydrogenase family, member 9	3	1	2
Ndufaf3	NADH dehydrogenase (ubiquinone) complex I, assembly factor 3	1	1	1
Ndufaf4	NADH dehydrogenase (ubiquinone) complex I, assembly factor 4	8	6	7
Ndufaf6	NADH dehydrogenase (ubiquinone) complex I, assembly factor 6	1	1	4
Ndufaf7	NADH dehydrogenase (ubiquinone) complex I, assembly factor 7	1	2	1
Sdhaf4	succinate dehydrogenase complex assembly factor 4	1	1	1
Uqcc1	ubiquinol-cytochrome c reductase complex assembly factor 1	4	1	4
Cox11	COX11 cytochrome c oxidase copper chaperone	7	6	7
Cox15	cytochrome c oxidase assembly homolog 15 (yeast)	7	4	4
Cox17	COX17 cytochrome c oxidase copper chaperone	2	2	2
Cox18	COX18 cytochrome c oxidase assembly factor	1	4	18
Sco1	SCO1 cytochrome c oxidase assembly protein	8	1	15
Atpaf1	ATP synthase mitochondrial F1 complex assembly factor 1	1	2	6

Red color depicts genes that contain Fe/S clusters.

Table S2. Serum iron and complete blood count (CBC) in mice in all experimental groups from global *Ttp* knock out mice.

Serum iron in male and female

	Tnfr1/2$^{-/-}$ RD		*Tnfr1/2*$^{-/-}$ ID		*Tnfr1/2*$^{-/-}$/*Ttp*$^{+/-}$ RD		*Tnfr1/2*$^{-/-}$/*Ttp*$^{+/-}$ ID		*Tnfr1/2*$^{-/-}$/*Ttp*$^{-/-}$ RD		*Tnfr1/2*$^{-/-}$/*Ttp*$^{-/-}$ ID	
	male	female	male	female	male	female	male	female	male	female	male	female
Serum iron (µg/dl)	107.1 ± 7.8	119.6 ± 9.1	31.3 ± 5.0	29.4 ± 5.6	117.3 ± 5.2	119.6 ± 2.9	19.2 ± 11.2	28 ± 11.8	121.9 ± 14.0	123.5 ± 19.4	32.8 ± 9.5	30.4 ± 2.4
UIBC (µg/dl)	252.2 ± 27.9	267.3 ± 22.2	400.6 ± 14.6	424.0 ± 15.9	166.6 ± 7.5	178.8 ± 8.0	421.5 ± 6.4	429.8 ± 20.1	293.4 ± 13.1	267.6 ± 19.9	422.4 ± 12.9	425.2 ± 19.3
Iron saturation (%)	31.0 ± 4.1	31.3 ± 2.6	7.2 ± 1.1	6.7 ± 1.5	41.4 ± 2.1	40.1 ± 1.7	4.3 ± 2.5	7.3 ± 2.8	28.9 ± 2.6	31.3 ± 4.0	7.1 ± 2.0	6.7 ± 0.6

CBC in male and female

§: difference between male and female

	Tnfr1/2$^{-/-}$ RD		*Tnfr1/2*$^{-/-}$ ID		*Tnfr1/2*$^{-/-}$/*Ttp*$^{+/-}$ RD		*Tnfr1/2*$^{-/-}$/*Ttp*$^{+/-}$ ID		*Tnfr1/2*$^{-/-}$/*Ttp*$^{-/-}$ RD		*Tnfr1/2*$^{-/-}$/*Ttp*$^{-/-}$ ID	
	male	female	male	female	male	female	male	female	male	female	male	female
Hgb (g/dl)	15.73 ± 0.32	15.38 ± 0.41	10.97 ± 0.83	10.98 ± 0.79	14.87 ± 0.21	15.05 ± 0.45	7.98 ± 0.13	7.83 ± 0.25	15.13 ± 0.23	15.57 ± 0.35	9.13 ± 0.79	9.07 ± 0.82
Hct (%)	62.43 ± 1.64	60.52 ± 1.02	46.02 ± 3.38	46.80 ± 2.81	51.73 ± 1.46	51.48 ± 0.83	32.83 ± 1.36	33.58 ± 1.49	59.07 ± 0.97	59.07 ± 1.53	37.48 ± 3.79	36.52 ± 2.73
MCV (fl)	54.78 ± 0.77	56.95 ± 0.68	42.48 ± 1.46	39.38 ± 1.05	51.53 ± 1.23	50.93 ± 0.48	39.37 ± 1.64	39.78 ± 0.56	52.02 ± 0.36	55.85 ± 0.63 §	40.43 ± 1.06	39.22 ± 0.66
WBC (x10^3/µl)	6.73 ± 1.25	12.28 ± 2.94	9.84 ± 2.34	10.82 ± 1.53	4.24 ± 0.95	2.41 ± 0.92	2.75 ± 0.95	2.21 ± 0.50	9.87 ± 1.05	13.30 ± 3.74	6.86 ± 1.86	14.55 ± 1.72 §
Plt (x10^3/µl)	768.8 ± 149.2	783.2 ± 82.2	1565.0 ± 197.6	1264.5 ± 237.4	992.4 ± 24.8	997.3 ± 22.3	1859.7 ± 294.6	1807.1 ± 326.5	956.3 ± 134.6	710.7 ± 113.4	2168.6 ± 360.8	1386.5 ± 198.5

No differences in serum iron parameters were detected in male vs female mice. Complete blood count raw data for males vs females showing that iron deficiency results in generally similar effects on hematopoietic system. n = 6 males and 6 females. Data expressed as mean ± SEM. Data analyzed with ANOVA with Tukey post hoc analysis; §$P < 0.05$.

Table S3. Serum iron and complete blood count (CBC) in cardiac-specific TTP knockout mice in all experimental groups.

Serum iron in male and female

	cs-*Ttp* WT RD		cs-*Ttp* WT ID		cs-*Ttp* KO RD		cs-*Ttp* KO ID	
	male	female	male	female	male	female	male	female
Serum iron (µg/dl)	80.7 ± 6.4	103.0 ± 7.9	29.0 ± 15.1	21.8 ± 6.3	106.5 ± 8.9	101.2 ± 7.1	27.9 ± 9.8	34.8 ± 11.6
UIBC (µg/dl)	223.3 ± 13.9	199.8 ± 18.9	547.3 ± 28.1	554.4 ± 41.5	185.7 ± 10.2	193.8± 19.2	454.6 ± 102.3	484.3 ± 45.6
Iron saturation (%)	26.7 ± 2.5	34.6 ± 3.0	5.1 ± 2.6	4.1 ± 1.4	36.5 ± 2.6	35.4± 3.7	7.1 ± 3.4	6.8 ± 2.4

CBC in male and female

§: difference between male and female

	cs-*Ttp* WT RD		cs-*Ttp* WT ID		cs-*Ttp* KO RD		cs-*Ttp* KO ID	
	male	female	male	female	male	female	male	female
Hgb (g/dl)	12.88 ± 0.83	13.97 ± 0.46	5.34 ± 0.55	6.13 ± 0.44	14.07 ± 0.82	14.54 ± 0.39	7.43 ± 0.97	6.24 ± 0.59
Hct (%)	44.14 ± 3.19	43.67 ± 1.10	19.51 ± 2.24	23.57 ± 2.01	43.87 ± 1.61	46.38 ± 1.03	26.25 ± 2.86	21.87 ± 2.96
MCV (fl)	46.95 ± 0.32	43.54 ± 0.49 §	35.73 ± 0.50	37.64 ± 0.65 §	43.75 ± 0.86	44.08 ± 0.79	36.94 ± 0.53	37.42 ± 0.58
WBC (x10^3/µl)	3.85 ± 0.74	4.07 ± 0.94	5.30 ± 1.08	5.59 ± 1.37	7.59 ± 0.80	3.68 ± 0.64 §	11.50 ± 2.83	2.53 ± 0.43
Plt (x10^3/µl)	418.6 ± 77.9	680.8 ± 95.8	2604.3 ± 198.8	3168.0 ± 168.1	831.8 ± 106.0	744.3 ± 137.6	2838.7 ± 255.0	2938.5 ± 301.1

No differences in serum iron parameters were detected in male vs female mice. Complete blood count raw data for males vs females showing that iron deficiency results in generally similar effects on hematopoietic system. n = 4-12 mice per group. Data expressed as mean ± SEM. Data analyzed with ANOVA with Tukey post hoc analysis for comparison between diets. Male vs female comparison were done with two-tailed T test; §$P < 0.05$.